Nanoscale

Accepted Manuscript

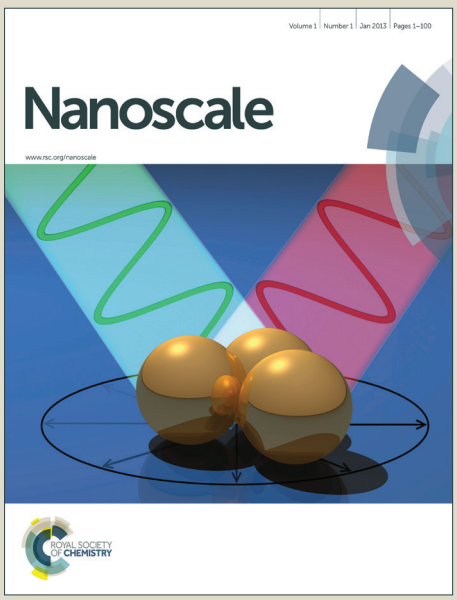

This is an *Accepted Manuscript*, which has been through the Royal Society of Chemistry peer review process and has been accepted for publication.

Accepted Manuscripts are published online shortly after acceptance, before technical editing, formatting and proof reading. Using this free service, authors can make their results available to the community, in citable form, before we publish the edited article. We will replace this *Accepted Manuscript* with the edited and formatted *Advance Article* as soon as it is available.

You can find more information about *Accepted Manuscripts* in the Information for Authors.

Please note that technical editing may introduce minor changes to the text and/or graphics, which may alter content. The journal's standard Terms & Conditions and the Ethical guidelines still apply. In no event shall the Royal Society of Chemistry be held responsible for any errors or omissions in this *Accepted Manuscript* or any consequences arising from the use of any information it contains.

ROYAL SOCIETY OF CHEMISTRY

www.rsc.org/nanoscale

Nanoscale

RSCPublishing

ARTICLE

Improving the efficiency of organic photovoltaics by tuning the work-function of graphene oxide hole transporting layers

Cite this: DOI: 10.1039/x0xx00000x

Emmanuel Stratakis[ab], Kyriaki Savva[b], Dimitrios Konios[a], Constantinos Petridis[a], and Emmanuel Kymakis*[a]

Received 00th January 2014,
Accepted 00th January 2014

DOI: 10.1039/x0xx00000x

www.rsc.org/

A facile, fast, non-destructive and roll to roll compatible photochemical method for the simultaneously partial reduction and doping of graphene oxide (GO) films through ultraviolet laser irradiation in the presence of Cl_2 precursor gas is demonstrated. The photochemical chlorinated GO-Cl films were fully characterized by XPS and Raman measurements, in which the grafting of chloride to the edges and the basal plane of GO was confirmed. By tuning the laser exposure time, it is possible to control the doping and reduction levels and therefore to tailor the work function (WF) of the GO-Cl layers from 4.9 eV to a maximum value of 5.23 eV. These WF values match the HOMO level of most polymer donors employed in OPV devices. Furthermore, high efficiency poly(2,7-carbazole) derivative (PCDTBT): fullerene derivative ($PC_{71}BM$) based OPVs with GO-Cl as the hole transporting layer (HTL) were demonstrated with power conversion efficiency (PCE) of 6.56 % which is 17.35 % and 19.48 % higher than the pristine GO and PEDOT:PSS based OPVs devices respectively. The performance enhancement was attributed to more efficient hole transportation due to the energy levels matching between the GO-Cl and the polymer donor.

Introduction

Organic photovoltaic (OPV) devices utilizing polymer-fullerene bulk heterojunctions (BHJs) have been widely studied due to their promising advantages over their traditional inorganic Si based counter-parts, including low cost fabrication on light weight, large area and flexible substrates and use of roll-to-roll (R2R) mass production techniques[1]. Recently, the research effort has been focused to the interface engineering of OPVs and especially to the introduction of buffer layers with electron blocking properties between the BHJ active layer and the transparent ITO electrode, in order to reduce recombination and leakage of current at the photoactive layer-electrode interface[2].

The highly doped poly(3,4 ethylenedioxythiophene): poly(styrenesulfonate) (PEDOT:PSS) is the most regularly used hole transporting layer (HTL) material for organic BHJ solar cells, because of its solution process ability, high work function, sufficient conductivity, and high optical transparency in the visible-NIR regime[3]. However, there are several drawback issues leading to OPV failure, which are directly related to the PEDOT:PSS. The acidic and hygroscopic nature of PEDOT:PSS corrodes both the ITO electrode[4] and the processing equipment[5] at elevated temperatures, and can introduce water into the active layer, degrading the performance and long-term stability of the OPV device.[6] In addition, the strong anisotropy in the conductivity of the spin coated PEDOT:PSS films originating from their lamellar structure, leads to inhomogeneous charge extraction in some locations and dead spots in others.[7] To overcome these drawbacks, several types of materials have been explored to serve as HTLs in BHJ solar cells, mainly focussing on metal oxide inorganic semiconductors[8]. However, the oxides are deposited using cost-intensive high vacuum techniques that are incompatible with low-cost solution-processable and r2r large area manufacturing of OPVs. So, it is obvious that the development of low cost and simply processable HTL materials compatible with OPV materials and r2r techniques is urgently demanded.

In this context, solution processable carbon nanotubes[9] and graphene based materials[10] were used as the HTL. In particular, spin coated graphene oxide (GO) derivatives have been studied as promising alternatives to PEDOT:PSS, due to their optical transparency, mechanical flexibility and compatibility with R2R production[11]. GO is a graphene sheet modified with oxygen functional groups in the form of epoxy and hydroxyl groups on the basal plane and various other types, such as carboxylic acid groups at the edges[12]. It can be produced by exfoliation of inexpensive graphite powders with strong oxidizing reagents[13]. The availability of reactive groups on both the basal plane and the GO sheets enables the manipulation of the size, shape and relative fraction of the sp^2 hybridized

Nanoscale Accepted Manuscript

domains of GO, allowing the tailoring of its optoelectronic properties[14].

However, the obtained performances are only comparable with the PEDOT:PSS based devices and not superior as would be expected due to the GO film higher transparency across the whole visible spectrum. The main barrier to higher performance enhancement is the work function (WF) of the as prepared GO film. The measured WFs are in the range of 4.7-4.9 eV[15] and do not match the highest occupied molecular orbital (HOMO) of the most commonly used electron donor materials in state of the art BHJ OPV devices, as in the PEDOT:PSS case (>5.1eV)[16]. Therefore, tuning of the GO WF with the polymer HOMO is needed. In this pathway, oxygen plasma treated and sulfated GO with increased WFs of 4.8 and 5.2 eV respectively were successfully utilized as the HTLs in OPVs[17]. Moreover, we recently demonstrated that spin coated GO films can be in-situ non-thermal reduced by femtosecond pulsed laser beam irradiation[18].

In this work, a novel approach of WF tuning of GO HTLs is demonstrated, based on laser-induced doping of GO. In particular, pulsed laser irradiation of ultrathin GO films in the presence of a dopant chloride (Cl_2) precursor gas, was employed for the simultaneous reduction and doping of GO. It is shown that the laser induced chloride atoms substitute the GO defects into both the edges and in the plane of the GO lattice[19]. In this way, the work function of irradiated layers can be tuned as a function of the laser exposure time. This process leads to a significant increase of the photocurrent and hence of the OPV devices performance mainly due to an increase in the hole mobility of the respective devices.

Results and Discussion

Characterization of photochlorinated GO films

The photochlorinated GO (GO-Cl) was investigated by XPS, UPS, and atomic force microscopy (AFM). Figure 1 compares typical XPS spectra of the pristine GO and GO-Cl films. It can be clearly seen that the intensity of the O1s peak relative to that of C1s is reduced while the characteristic Cl2p, due to chloride bonds, appears after the photoclorination process. The XPS results clearly indicate that simultaneous photoreduction and Cl doping of the GO nanosheets takes place.

Figures 1b present in high resolution the respective C1s peaks of GO and GO-Cl, consisting of three kinds of components assigned to C–O (hydroxyl and epoxy), C=O (carbonyl), and C–(O)–O (carboxyl) functional groups[20]. Upon photochlorination, the C-O/C-C intensity ratio decreases from 1.09 to 0.60 while the Cl2p/C1s intensity ratio becomes equal to 0.17. In particular, the C1s spectrum of as-prepared GO sheets shows an additional peak at higher binding energies, corresponding to large amounts of sp^3 carbon with C-O bonds, carbonyls (C=O), and carboxylates (O-C=O).[21].

Figure 1c shows the high-resolution Cl2p spectra of the GO-Cl film, confirming the Cl_2 doping in the GO lattice. The Cl2p spectra can be fitted in two nonequivalent chlorine sites from the A) 3/2 and B) 1/2 levels. The more intense peak A was close to 200 eV corresponding to Cl-C covalent bonds at the edges, while the less intense peak B at 201.7 eV corresponds to the Cl–C=O groups[22]. The above findings indicate enhancement of the doping efficiency upon increasing the number of the GO oxygen groups, suggesting that Cl-doping most likely occurs at the edges and defect sites[23].

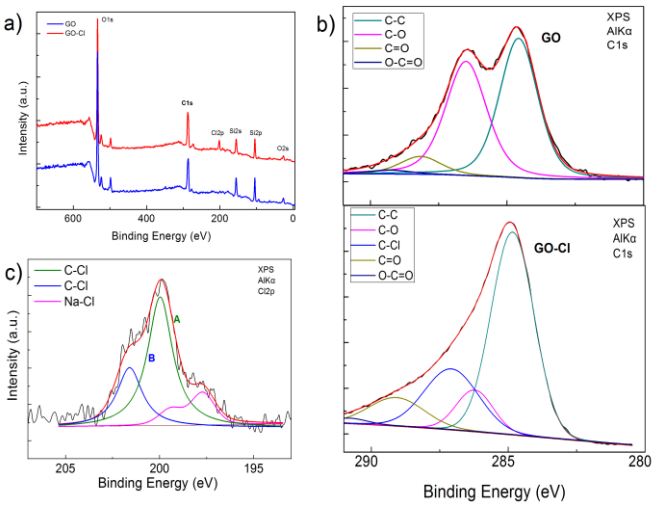

Figure 1: (a) XPS survey spectra and (b), high-resolution XPS C1s spectra and c) high resolution Cl2p XPS spectra of GO and GO-Cl films.

Tuning of the laser source key parameters can lead to a respective tuning of Cl_2 doping level of the GO. In particular, this can take place upon increasing the laser power (P) in the range from 10 to 50 mW or increase of number of pulsed (N_p) at a certain P, giving rise to a corresponding decrease of the doping level. Figure 2a shows that the I(C-C)/I(C-O) ratio, which corresponds to the GO reduction degree, increases upon increasing the Np, while the I(Cl2p)/I(C1s) ratio, which corresponds to Cl_2 doping, decreases. The maximum introduction of Cl-groups attained was ~11.3 atom % as can be estimated by the ratio of the Cl2p to the C1s peak areas after considering the atomic sensitivity factors for Cl2p and C1s.

The work-function of the respective GO-Cl layers determined by ultraviolet photoelectron spectroscopy (UPS), and scanning kelvin probe microscopy (SKPM) for Np values of 1-60 and are presented in Fig. 2b. It was observed that the WF rises with increased exposure, and tends to saturate at 5.23 eV for Np=60. As can be seen in the respective UPS spectra of Fig. 2c, this value is much higher than the respective WFs measured for GO (4.9 eV). The maximum WF is obtained at the point, which both the reduction and the doping rates start to significantly increase and decrease respectively. Therefore, as can be also seen from the inset of Fig.2b, the WF increase is most likely due to a synergetic effect of the chloride doping and the partial reduction processes.

It is evident that laser radiation causes partial reduction of the GO sheets while at the same time chlorine molecules split into highly reactive radicals and react with the GO lattice via a free

Nanoscale Accepted Manuscript

This journal is © The Royal Society of Chemistry 2014

radical addition reaction. Under these conditions, tuning of the GO WF can be achieved by the formation of surface $C^{\delta+}$-$Cl^{\delta-}$ dipoles with different electronegativity (2.55 for C compared to 3.16 for Cl).

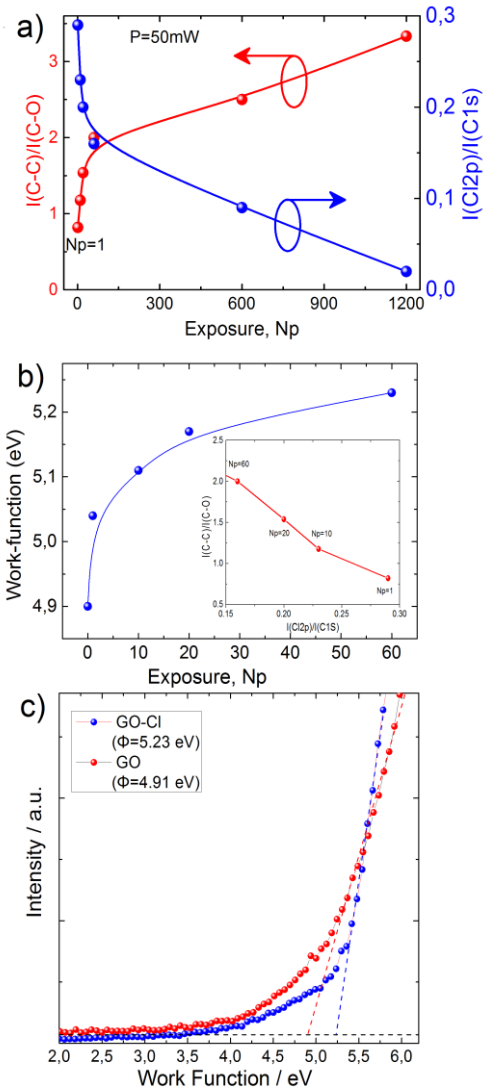

Figure 2: a) GO reduction and doping levels as a function of Np b) Work function of GO-Cl films as a function of the Np exposure. The inset shows the dependence of Cl2 doping (I(Cl2p)/I(C1S) with the reduction degree ((I(C-C)/I(C-O)) c) UPS spectra of the GO and GO-Cl (Np=60) films)

As shown in Fig. 3a, such dipoles can be formed by chlorine atoms in Cl-C covalent bonds at the edges and/or Cl–C=O groups located outside the graphene basal plane[24,25]. The induced polar character of C-Cl bonds is responsible for the downward shift of the Fermi level in the valence band of GO-Cl, and the subsequent increase in the work function from 4.9 eV in GO to 5.23eV in GO-Cl (Fig. 3b)[25,26]. In addition, the charge rearrangement by the electron drawing towards chlorine atoms, increase the number of hole charge carriers in the conjugated sp^2 network of GO-Cl, enhancing its p-type behavior[27]. Therefore, the strength of the out of plane dipole moment in the GO, and thus the WF can be tuned by a) the variation of the overall oxygen content, realized by partial reduction and b) the replacement of oxygen atoms with chloride ones with higher electronegativity upon doping.

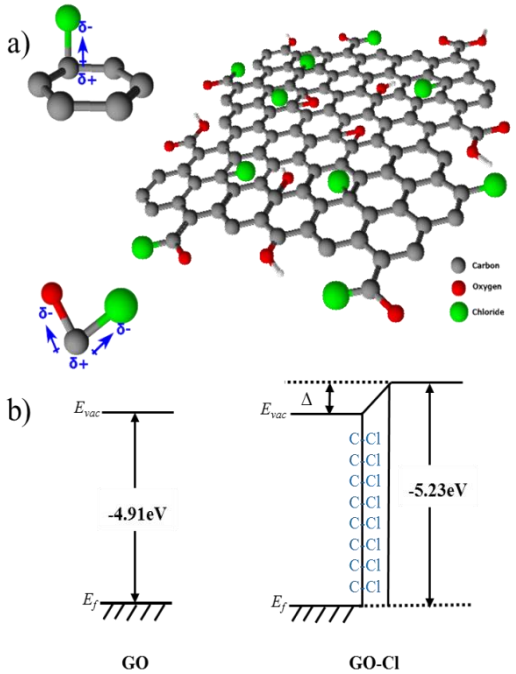

Figure 3: a) 3D chemical structure of the photochlorinated GO, illustrating the formation of dipoles by chlorine atoms in Cl-C covalent bonds at the edges and/or Cl–C=O groups located outside the graphene basal plane. b) Schematic energy level diagram showing the effect of polar C-Cl bonds on the work function.

Photovoltaic characteristics

To explore the effects of the photochlorination of the GO layer on device performance, OPVs with the conventional device structure glass /indium tin oxide (ITO)/ HTL/ polymer: $PC_{71}BM$/TiO_x/Al, where fabricated. The HTL layers compared were PEDOT:PSS, GO and GO-Cl. The device structure and the energy level diagrams of the different materials used in the

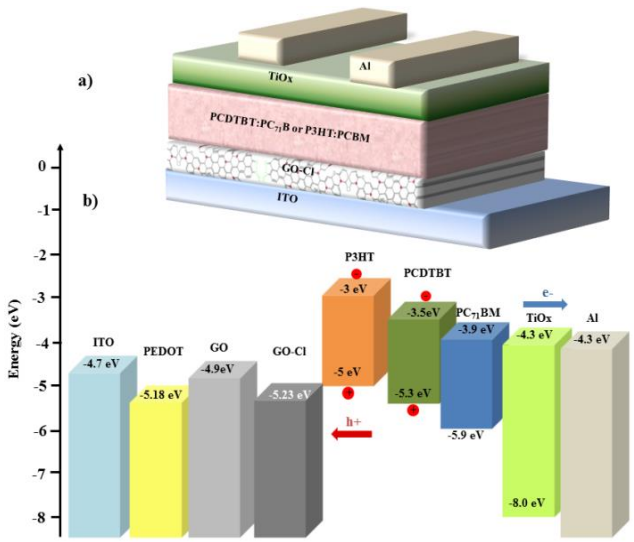

Figure 4: Schematic illustration of the BHJ OPV device with GO-Cl HTL (b) The energy level diagram depicting the relevant energy levels under flat band conditions of all materials used in the OPV cells studied and not the actual interfaces.

Nanoscale Accepted Manuscript

fabrication are shown in Figure 4a and 4b.

Before analyzing the photovoltaic characteristics, it is important to describe the functionality of the HTL during the device operation. The solar light irradiates the photoactive layer through the HTL/ITO electrode side, while the active layer absorbs photons to produce excitons. The photo-excited excitons dissociate at the polymer-fullerene interface into electrons in the lowest unoccupied molecular orbital (LUMO) of the fullerene acceptor, and holes in the highest occupied molecular orbital (HOMO) of the polymer donor. Therefore, the HOMO level of the polymer donor should be ideally equal to the WF of the HTL, so that the holes can be readily transported to the ITO electrode through the HTL. In this context, two different polymer donors a) P3HT with HOMO of 5 eV and b) PCDTBT with HOMO of 5.3 eV were utilized, in order to examine the influence of the GO-Cl HTL WF on the photovoltaic characteristics. Reference devices incorporating the PEDOT:PSS and pristine GO as the HTL were also fabricated for comparison. It should be noted that the optimum thickness of the GO film is found to be around 3.4 nm for both GO and GO-Cl HTLs. This finding is in disparity with the first report of GO based HTLs, where the GO thin films with a thickness of 2 nm gave the highest efficiency[11], but in agreement with our previous studies[9] and recent studies of plasma treated GO HTLs, in which the same spinning conditions of the GO films, resulted in 1 and 3 nm thin films on mica and ITO substrates respectively[17]. This effect may also be caused by the different lateral dimensions of GO flakes employed.

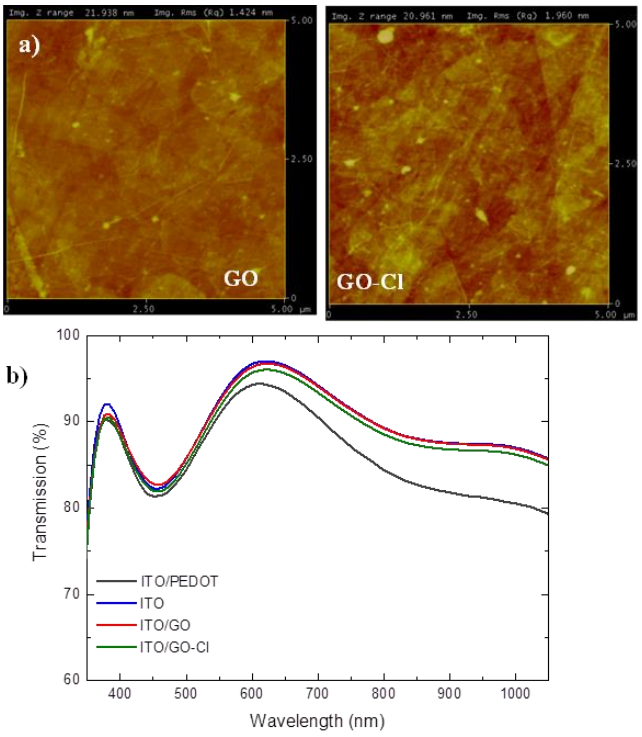

Figure 5: a) 5μm x 5μm AFM images of the GO (left) and the GO-Cl layer (right) with RMS roughness of 1.424 and 1.96 nm on ITO/glass substrates b) Transmission spectra of GO and GO-Cl films spin coated on ITO/glass. The spectra of ITO glass and ITO glass coated with PEDOT:PSS are also shown.

Finally it is important to note that the mean roughness of both GO and GO-Cl HTLs is comparable as indicated by AFM measurements (Fig. 5). This suggests that the photochlorination process does not significantly affect the HTL film morphology.

Figure 6 shows the typical illuminated current density-voltage (J-V) curves of the PCDTBT:$PC_{71}BM$ OPV devices with PEDOT:PSS, GO and GO-Cl (prepared at different exposure times) as the HTLs. As it can be seen in the J–V curves and the summarized photovoltaic parameters in Table 1, device performance is significantly enhanced by the photochlorination of the GO film and strongly depends on the WF of the GO-Cl layer. Indeed, the increase of the WF of GO-Cl films from 4.9 to 5.23 eV leads to a PCE of 6.56 % which is 17.35 % and 19.48 % higher than the pristine GO and PEDOT:PSS based OPVs devices respectively. The PCE enhancement achieved via the GO film photochlorination is primarily a result of increased $J_{SC,}$ which is proportional to the WF increase of the GO-Cl films.

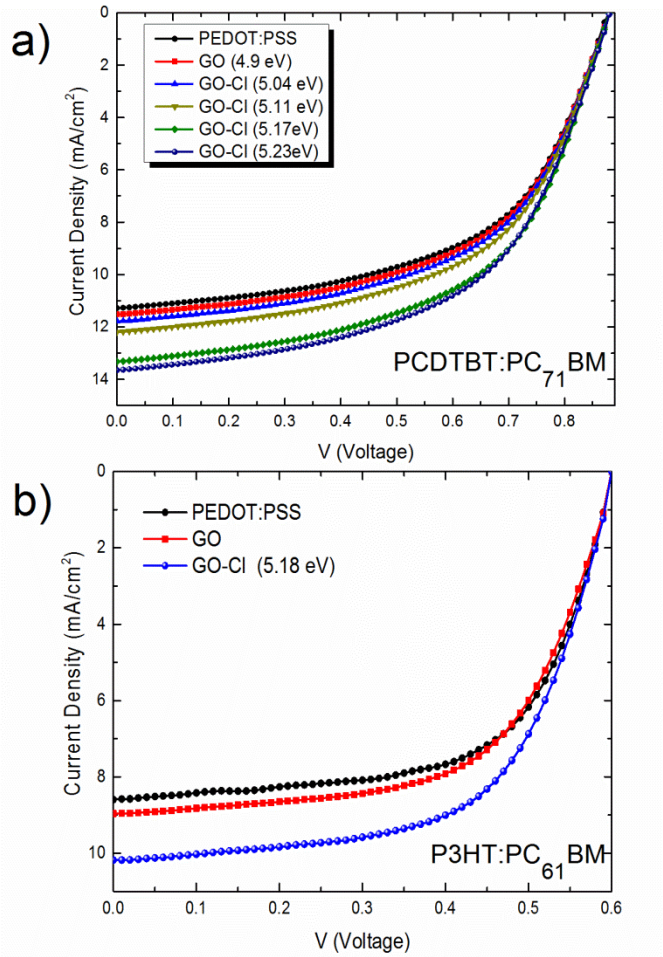

Figure 6: J-V characteristics of a) PCDTBT:$PC_{71}BM$ and b) P3HT:$PC_{61}BM$ photovoltaic devices with different HTLs under simulated AM 1.5, 100 mW/cm^2 solar irradiation

This J_{SC} increase cannot be attributed to enhanced optical transmittance, since there was practically no difference in transparency between the pristine and photochlorinated GO HTLs (Figure 5b). Also, it should be noted that, the pristine

Nanoscale Accepted Manuscript

This journal is © The Royal Society of Chemistry 2014

GO based OPV slightly outperforms the PEDOT: PSS due to a small increase of J_{SC}. Such increase may be attributed to the improved hole transportation due to the 2D nature of the HTL. Our results suggest that the photocurrent enhancement can be explained by an improvement on the hole transport efficiency facilitated by the perfect match of GO-Cl WF with the HOMO level of the polymer. To validate this presumption, hole-only devices with the structure: ITO/HTL/PCDTBT:$PC_{71}BM$/MoO_3/Au were fabricated for all different types of devices. The hole mobility was estimated from the *J*–V characteristics at low voltage region, where the current is described by the Mott-Gurney square law[28]:

$$J_{SCLC} = \frac{9}{8}\varepsilon_o\varepsilon_r\mu_h\frac{V^2}{L^3}$$

where ε_o is the permittivity of free space, ε_r is the dielectric constant of the active layer, μ_h is the hole mobility, and L is the active layer film thickness[29].

Table 1: Summary of the photovoltaic parameters of the fabricated OPVs with a) PCDTBT:$PC_{71}BM$ and b) P3HT:$PC_{61}BM$ active layers using different HTLs (The data was averaged from ten devices)

HTL	J_{SC} (mA/cm^2)	V_{OC} (V)	FF (%)	PCE (%)
PCDTBT:$PC_{71}BM$				
PEDOT:PSS	11.27	0.88	55.3	5.49
GO 4.9 eV	11.52	0.88	55.1	5.59
GO-Cl 5.04 eV	11.78	0.88	55.1	5.71
GO-Cl 5.11 eV	12.19	0.88	55.2	5.92
GO-Cl 5.17 eV	13.32	0.88	55.1	6.46
GO-Cl 5.23 eV	13.65	0.88	54.7	6.56
P3HT:$PC_{61}BM$				
PEDOT:PSS	8.59	0.6	62.7	3.23
GO	8.96	0.6	61.0	3.28
GO-Cl 5.23 eV	10.18	0.6	61.3	3.74

It should be noted that the obtained hole mobilities refer to the complete device including the active and the HTLs. The hole mobilities of the devices prepared with PEDOT:PSS, GO and GO-Cl (5.23 eV) as the HTLs, respectively are calculated from the currents in the square law region to be 9.64 x 10^{-5}, 1.2 x 10^{-4} and 2.35 x 10^{-4} cm^2 V^{-1}s^{-1} respectively.Therefore, it is more than clear that the hole mobility increases as the GO-Cl WF increases, leading to higher PCEs due to improve hole transport. Further support of the enhancement effect of GO-Cl HTLs is the observation that OPV devices incorporating GO HTLs that were laser irradiated without the presence of chloride, exhibit PCEs comparable with that of devices incorporating pristine GO HTLs. Moreover, the dark current density in reverse bias of the OPVs with GO-Cl is one order of magnitude lower than that of the OPVs with pristine GO HTLs, resulting in a higher diode rectification ratio and therefore better hole collection and electron blocking behaviour. Therefore, it can be concluded that only the simultaneous partial reduction and chlorination of the GO films, lead to increased WF, and hence PCE.

A similar but less impressive performance enhancement was observed in OPVs with the P3HT polymer. As shown in Fig.5b, the devices with GO-Cl (5.23 eV) as the HTL, exhibited a PCE of 3.74 %, which is 14% higher compared with the GO-based OPV device. This enhancement is lower than that obtained in the PCDTBT OPV device. This discrepancy in PCE enhancement is possibly due to the fact that the energy barrier between the HOMO of the PCDTB (5.3 eV) and the WF of GO-Cl (5.23 eV) is only 0.07 eV. While, in the P3HT (HOMO of 5 eV) case, the corresponding energy barrier is 0.23 eV. This reduced barrier in the case of PCDTBT enables more efficient charge transport and reduced recombination at the hole transport and photoactive layers, giving rise to higher PCE enhancement. Therefore, it can be concluded that tuning of the GO-Cl WF with respect to the energy levels of the polymer donor is the main performance enhancement factor. Indeed, the higher PCE enhancement observed using PCDTBT compared to P3HT donor can be attributed to the perfect match of the GO-Cl WF and LUMO taking place in the former case. Optical or morphological side effects can be neglected, since the measured roughness and optical transmission of the pristine and the photochlorinated GO layers are comparable.

The OPVs with GO-Cl as the HTL exhibit significant higher lifetime stability when exposed to continuous solar illumination in air compared with OPVs using PEDOT:PSS. OPVs were tested under prolonged irradiation without any encapsulation. While OPVs with PEDOT:PSS as the HTL die after 20h, OPVs fabricated with GO or GO-Cl HTLs preserve more than 70% and 50% of its initial PCE for over 25h and 45 h respectively[11b]. This result is due to the fact that PEDOT:PSS is spin coated from highly acidic suspension (pH~1), which erodes ITO and causes indium migration into the photoactive layers. Also, water molecules can readily penetrate into the hygroscopic PEDOT:PSS layer, resulting in degraded device performance[30]. Thus, the GO-Cl does not only enhance the device PCE but also act against fast degradation of the device, offering a superior alternative HTL material.

Finally, it is important to note that the presented technique ensures low cost, since it is a room temperature process and applicable to flexible and light-weight substrates, and therefore compatible with large industrial roll to roll manufacturing of OPVs. A GO ink is printed onto flexible plastic foils using standard industrial inkjet printers, then the GO film can be in-situ photochlorinated using a scanning laser beam. Furthermore, the technique can be applied to other organic electronic devices, in which tuning of the graphene ink electronic properties is desirable

Conclusions

In summary, ultraviolet laser irradiation in a chlorine gas medium was successfully employed as a facile and catalyst-free approach to prepare photochlorinated GO films with controllable reduction and doping levels, and thus work function. In effect, the resultant GO-Cl has been demonstrated to be an excellent HTL material for OPVs, significantly

Nanoscale Accepted Manuscript

outperforming the reference PEDOT:PSS and pristine GO HTLs. This is attributed to its increased work function, which perfectly matches with the HOMO level of the PCDTBT, ensuring an ohmic contact at the interface. This new technique can employ other dopants for not only the increase but also the decrease of the GO work function, aiming to its use as the electron transport layer, opening new avenues for the development of an all graphene based OPVs.

Experimental section

GO film fabrication

Graphite oxide was synthesized by the modified Hummers method and exfoliated to give a brown dispersion of GO under ultrasonication[31]. The resulting GO was negatively charged over a wide pH condition, as the GO sheet had chemical functional groups of carboxylic acids. GO solution in ethanol (0.5 mg/ml) at pH 3.3 was dropped after an oxygen plasma treatment for 2 min in order to make the ITO surface hydrophilic. The GO solution was maintained for a waiting period of 2 min and was then spun at 3000 rpm for 30 s, followed by 30 min baking at 100 °C inside a nitrogen-filled glove box. The thickness of the films was analogous to the number of spinning repetitions; a film thickness of 3.4 nm was obtained with two successive coatings.

Photochemical doping and reduction of GO films

The as-spun GO layers on ITO/glass substrates were subjected to irradiation by a KrF excimer laser source emitting 20 ns pulses of 248 nm at 1Hz repetition rate that was translated onto the film area. For uniform exposure of the whole sample to laser radiation, a top-flat beam profile of 20×10 mm^2 was obtained using a beam homogenizer. The whole process took place into a vacuum chamber at 50 Torr Cl_2 gas pressure maintained through a precision micro valve system. Different combinations of laser powers (P) and number of pulses (N_P) were tested in an effort to optimize the photochemical functionalization processes. In a typical experiment, the sample was irradiated at a constant P with Np = 10, 20, 30, 40, 50, 60, 120, 600 and 1200, corresponding to different photochemical reaction times.

Device fabrication

The photovoltaic devices reported were fabricated on 15 mm by 15 mm indium–tin-oxide (ITO) glass substrates with a sheet resistance of 15Ω/sq. The impurities are removed from the ITO glass through a 3-step cleaning process. GO with different thicknesses were spin casted as described previously. Next, a photoactive layer consisting of a P3HT:PCBM (1:1 wt.% ratio, 220 nm thick) or a PCDTBT:$PC_{71}BM$ (1:4 wt.% ratio, 80 nm thick) blend was spin coated on the HTL from a dichlorobenzene (o-DCB) or 1:4 ratio dichlorobenzene:chlorobenzene solution respectively at 1000 rpm. Both solutions were stirred for at least 72 hours at 80°C before used. The P3HT-PCBM devices were then post-annealed at 160 °C for 15 min in a glove box under nitrogen atmosphere.

For the PCDTBT:$PC_{71}BM$ devices, a TiOx electron transporting interlayer was dissolved in methanol (1:200) and then spin-coated to a thickness of approximately 10 nm (6000 rpm, 40 s). Finally, a 100 nm thick Al layer was deposited by thermal evaporation through a shadow mask to define an active area of 6 mm^2. Devices were encapsulated for testing in air with a UV-curable epoxy and covered with a glass slide and were fixed on top of an aperture having exact the same dimensions as the active area (overlap of ITO and Al electrodes) during all measurements.

Microscopic and Spectroscopic Characterization

The by UV-VIS absorption spectra of the samples were recorded using a Shimadzu UV-2401 PC spectrophotometer over the wavelength range of 400–1000 nm. The morphology of the surfaces was examined by field emission scanning electron microscopy (FE-SEM; JEOL JSM-7000F) and by atomic force microscopy (AFM; Digital Instruments NanoScope IIIa). X-ray photoelectron spectroscopy (XPS) measurements were carried out in a Specs LHS-10 Ultrahigh Vacuum (UHV) system. The XPS spectra were recorded at room temperature using unmonochromatized AlKa radiation under conditions optimized for maximum signal (constant ΔE mode with pass energy of 36 eV giving a full width at half maximum (FWHM) of 0.9 eV for the Au 4f7/2 peak). The analyzed area was an ellipsoid with dimensions 2.5 x 4.5 mm^2. The XPS core level spectra were analysed using a fitting routine, which allows the decomposition of each spectrum into individual mixed Gaussian-Lorentzian components after a Shirley background subtraction. The ultraviolet photoelectron spectroscopy (UPS) spectra were obtained using HeI irradiation with hν = 21.23 eV produced by a UV source (model UVS 10/35). During UPS measurements the analyser was working at the Constant Retarding Ratio (CRR) mode, with CRR = 10. The work function was determined from the UPS spectra by subtracting their width (i.e. the energy difference between the analyzer Fermi level and the high binding energy cutoff), from the HeI excitation energy. For these measurements a bias of −12.30 V was applied to the sample in order to avoid interference of the spectrometer threshold in the UPS spectra. All the work function values obtained by UPS were calibrated with scanning kelvin probe microscopy (SKPM) measurements. The relative error is 0.02 eV.

Device Parameters

Current–voltage (I–V) measurements were performed at room temperature using an Agilent B1500A Semiconductor Device Analyzer. For photovoltaic characterization the devices were illuminated with 100 $mWcm^{-2}$ power intensity of white light using an Oriel solar simulator with an AM1.5 filter through the glass/ITO side. A reference monocrystalline silicon solar cell from Newport was used to calibrate the lamp. X-ray photoelectron spectroscopy (XPS) was used to probe and quantify the level of dopants introduced into the GO lattice.

Nanoscale Accepted Manuscript

 This journal is © The Royal Society of Chemistry 2014

Acknowledgements

The research leading to these results has received funding from the European Union Seventh Framework Programme under grant agreement n°604391 Graphene Flagship.

Notes and References

[a] Center of Materials Technology & Photonics and Electrical Engineering Department, School of Engineering School of Engineering, Technological Educational Institute (TEI) of Crete, Heraklion, Crete, Greece. Tel: +30 2810379895; E-mail: kymakis@staff.teicrete.gr
[b] Institute of Electronic Structure and Laser (IESL), Foundation for Research and Technology-Hellas (FORTH), & Dept. Of Materials Science and Technology, Univ. Of Crete, Heraklion, Crete, Greece.

[1] a) H. Y. Chen, J. H. Hou, S. Q. Zhang, Y. Y. Liang, G. W. Yang, Y. Yang, L. P. Yu, Y. Wu, G. Li, *Nature Photon.*, 2009, **3**, 649.; b) G. Zhao, Y. He, Y. Li, *Adv. Mater.*, 2010, **22**, 4355. ; c) E. Stratakis, E. Kymakis, *Mater. Today*, 2013, **16**, 133 ; d) K.D.G.I. Jayawardena, L.J. Rozanski, C.A. Mills, M.J. Beliatis, N.A. Nismy, S.R.P. Silva, *Nanoscale*, 2013, **5**, 8411.; e) C. J. Brabec , S. Gowrisanker, J.J.M. Halls, D. Laird, S.J. Jia , S.P. Williams, *Adv. Mater.*, 2010, **22**, 3839.

[2] a) R. Steim, F.R. Koglera, C.J. Brabec, *J. Mater. Chem.*, 2010, **20**, 2499.; b) H. L. Yip and A. K. Y. Jen, *Energy Environ. Sci*., 2012, **5**, 5994-6011; c) R. Po, C. Carbonera, A. Bernardia, N. Camaioni, *Energy Environ. Sci*., 2011,**4**, 285.

[3] F. Zhang, M. Ceder, O. Inganas, *Adv. Mater.*, 2007, **19**, 1835.

[4] a) H. Yan, P. Lee, N. R. Armstrong, A. Graham, G. A. Evmenenko, P. Dutta, T. J. Marks, *J. Am. Chem. Soc.*, 2005, **127**, 3172. b) M. Jorgensen, K. Norrman, F. C. Krebs, *Sol. Energy Mater. Sol. Cells*, 2008, **92**, 686.

[5] X. H. Yang, F. Jaiser, B. Stiller, D. Neher, F. Galbrecht, U. Scherf, *Adv. Funct. Mater*., 2006, **16**, 2156.

[6] a) J. Van de Lagemaat, T. M. Barnes, G. Rumbles, S. E. Shaheen, T. J. Coutts, C. Weeks, I. Levitsky, J. Peltola, P. Glatkowski, *Appl. Phys. Lett.*, 2006, **88**, 2333503.; b) F. So, D. Kondakov, *Adv. Mater.*, 2010, **22**, 3762

[7] a) A. W. Hains, T. J. Marks, *Appl. Phys. Lett.*, 2008, **92**, 1. ; b) M. Kemerink, S. Timpanaro, M. M. de Kok, E. A. Meulenkamp, F. J. Touwslager, *J. Phys. Chem. B.*, 2004, **108**, 18820.

[8] a) A. Garcia, G. C. Welch, E. L. Ratcliff, D. S. Ginley, G. C. Bazan, D. C. Olson, *Adv. Mater.* 2012, **24**, 5368 b) M. S. White, D. C. Olson, S. E. Shaheen, N. Kopidakis, D. S. Ginley, *Appl. Phys. Lett.*, 2006, **89**, 143517.; c) R. Po, C. Carbonera, A. Bernardi and N. Camaioni, *Energy Environ. Sci.*, 2011, **4**, 285-310.; c) M.T. Greiner, M.G. Helander, W.M. Tang, Z.B. Wang, J. Qiu, Z.H. Lu, *Nat. Mater*., 2012, **11**, 76. ; d) M. Vasilopoulou, A. Soultati, D.G. Georgiadou, T. Stergiopoulos, L.C. Palilis, S. Kennou, N.A. Stathopoulos, D. Davazoglou, P. Argitis, *J. Mater. Chem. A*, 2014, **2**, 1738.

[9] E. Kymakis, M.M. Stylianakis, G.D. Spyropoulos, E. Stratakis, E. Koudoumas, C. Fotakis, *Sol. Energy Mater. Sol. Cells*, 2012, **96**, 298

[10] J. Liu, M. Durstock, L. Dai., *Energy Environ. Sci*., 2014, **7**, 1297

[11] a) S. S. Li, K. H. Tu, C. C. Lin, C. W. Chen, M. Chhowalla, *ACS Nano* 2010, **4**, 3169; b) E. Stratakis, M.M. Stylianakis, E. Koudoumas, E. Kymakis, *Nanoscale*, 2013, **5**, 4144.; c) H. P. Kim, A. R. M. Yusoff, J. Jang, *Sol. Energy Mater. Sol. Cells*, 2013, **110**, 87.; d) X.D. Liu, H. Kim and L. J. Guo, *Org. Electron*., 2013, **14**, 591–598

[12] W.W. Cai, R. D. Piner, F. J. Stadermann, S. Park, M. A. Shaibat, Y. Ishii, D. X. Yang, A. Velamakanni, S. J. An, M. Stoller, J. H. An, D. M. Chen, R. S. Ruoff, *Science*, 2008, **321**, 1815.

[13] W. S. Hummers and R. E. Offeman, *J. Am. Chem. Soc*., 1958, **80**, 1339

[14] a) D. R. Dreyer, S. J. Park, C. W. Bielawski, R. S. Ruoff, *Chem. Soc. Rev*., 2010, **39**, 228; b) P. Matyba, H. Yamaguchi, M. Chhowalla, N. D. Robinson, L. Edman, ACS Nano, 2010, **5**, 574; c) K. P. Loh, Q. Bao, G. Eda, M. Chhowalla, *Nat. Chem.*, 2010, **2**, 1015

[15] a) J. Liu , Y. Xue, Y. Gao, D. Yu, M. Durstock, L. Dai, *Adv. Mater*. 2012, **24**, 2228.; b) B. R. Lee, J. W. Kim, D. Kang, S. Ko, H. J. Lee, J. Y. Kim, H. S. Shin, M. H. Song, ACS Nano, 2012, **6**, 2984.

[16] C. L. Chochos, S. A. Choulis, *Prog. Polym. Sci*., 2011, **36**, 1326

[17] a) D. Yang, L.Y. Zhou, L.C. Chen, B. Zhao, J. Zhang, C. Li, *Chem. Commun.* 2012, **48**, 8078 ; b) J. Liu, Y. H. Xue, L. M. Dai, *J. Phys. Chem. Lett.* 2012, **3**, 1928

[18] E. Kymakis, K. Savva, M.M. Stylianakis, C. Fotakis, E. Stratakis, *Adv. Funct. Mater*., 2013, **23**, 2742.

[19] B. Li, L. Zhou, D. Wu, H. Pang, K. Yan, Y. Zhou, Z. Liu, *ACS Nano*, 2011, **5**, 5957.

[20] D.R. Dreyer, S. Park, C.W. Bielawski , R.S. Ruoff, *Chem. Soc. Rev*., 2010 , **39** , 228.

[21] S. Stankovich, D. A. Dikin, R.D. Piner, K.A. Kohlhaas, A. Kleinhammes, Y. Jia, Y. Wu, S.T. Nguyen, R.S. Ruoff, *Carbon*, 2007, **45**, 1558.

[22] D.-W. Wang, K.-H. Wu , I.R. Gentle, G.Q. Lu ,*Carbon* 2012, 50, 333

[23] a) X. Wang, X. Li, L. Zhang, Y. Yoon, P.K. Weber, H. Wang, J. Guo, H. Dai, *Science*, 2009, **324**, 768.; b) J.L. Bahr, J.P. Yang, D.V. Kosynkin, M.J. Bronikowski, R.E. Smalley, J.M. Tour, *J. Am. Chem. Soc*., 2001, **123**, 6536.

[24] P.V. Kumar, M. Bernardi, J.C. Grossman, *ACS Nano*, 2013, **7**, 1638.

[25] J.-Y. Kim, W. H. Lee, J. W. Suk, J. R. Potts, H. Chou, I. N. Kholmanov, R. D. Piner, J. Lee, D. Akinwande and R. S. Ruoff, *Adv. Mater*., 2013, **16**, 2308

[26] K.C. Kwon, K.S. Choi, Y. Kim, *Adv. Funct. Mater*. 2012, **22**, 4724

[27] J.K. Wassei, K.C. Cha, V.C. Tung, Y. Yang, R. B. Kaner, J. *Mater. Chem*., 2011, **21**, 3391

[28] M. Y. Chiu, U. Jeng, C. H. Su, K. S. Liang,K. H. Wei, *Adv. Mater.*, 2008, **20**, 2573.

[29] V. Shrotriya, E. H.-E. Wu, G. Li, Y. Yao, Y. Yang, *Appl. Phys. Lett*., 2006, **88**, 064104.

[30] M. Jørgensen, K. Norrman and F. C. Krebs, Sol. Energy Mater. Sol. Cells, 2008, 92, 686

[31] D. Li, M.B. Müller, S. Gilje, R.B. Kaner, G.G. Wallace, *Nat. Nanotechnol.*, 2008, **3**, 101.

Nanoscale Accepted Manuscript